Middle East Journal of Applied Science & Technology
Vol.5, Iss.2, Pages 09-16, April-June 2022

A Novel Undistorted Image Fusion and DWT Based Compression Model with FPGA Implementation for Medical Applications

M. Mohankumar[1], S. Akilan[2], B. Hariprasath[3], R. Ariprasath[4] & S. Dhanu Dharsan[5]

[1-5]*Department of Electronics and Communication Engineering, Sri Eshwar College of Engineering, Coimbatore, Tamilnadu, India.*

DOI: http://doi.org/10.46431/MEJAST.2022.5202

Article Received: 12 February 2022 *Article Accepted: 18 April 2022* *Article Published: 23 May 2022*

ABSTRACT

The usage of a fused image and compressed model in a VLSI implementation is demonstrated. In this study, distortion correction is also considered. In distortion correction models, least-squares estimate is utilized. The technique of picture fusion is widely employed in medical imaging. Many pictures are obtained from various sensors (or) multiple images are captured at different times by one sensor in the image fusion approach. CT scans give useful information on denser tissue with the least amount of distortion. The information obtained from a magnetic resonance imaging (MRI) of soft tissue with significant distortion is useful. The DWT-based image fusion approach employs discrete wavelet transforms, a novel multi-resolution analytic tool. Back mapping expansion polynomial is used to reduce computer complexity. Using 0.18um technology, the suggested VLSI design achieves 218MHz with 1480 logical components.

Keywords: *Distortion correction, DWT, Image fusion, Horner's Algorithm, Back mapping.*

1. Introduction

Image fusion is widely employed in various industries, including medical imaging, surveillance applications, biometrics, and so on. It's the process of integrating similar data from two (or more) photos into a single image. After that, the final image has more information than the input photos. Various sorts of sounds distort multi-resolution images obtained by various image fusion cameras. Before processing, a cost-effective VLSI architectural technique for distortion correction should be used [1].

Distortion can be caused by a variety of variables, such as the over-the-band effect in camera lenses, radial (or) barrel distortion, and so on. Traditionally, distortion correction is performed only after the image has been taken, and a separate image processing system is required for fusion. In this paper, we present a circuit architecture that is linked to end-user camera equipment. The back-mapping technique reduces distortion correction.

A polar coordinate transformation can be converted to Cartesian coordinates using Horner's technique [2]. Back mapping provides for less hardware and power usage, as well as a reduction in computational complexity. Circuit for linear interpolation, the proposed architecture in this study is meant to accomplish minimal power and memory needs, as the circuit employs a SOC-based RAM bank. When working with raw medical photos, distortion reduction is a must. Large discrepancies can be caused by even minor distortions. As a result, pre-processing the image is required before combining numerous photos. In this situation, barrel distortion has ruined the photographs [3]. In this stage, we will repair the image in two steps.

STEP-1: Converting CIS pixels to DIS pixels.

STEP-2: The intensity is calculated via linear interpolation, each pixel in CIS. Initially, this transformation converts all pixels in the image's rectangular coordinates to polar coordinates. Back mapping is therefore required to lessen the complexity of computations and coordinate transformations (from polar to rectangular). The angle of the lens from the reference plane is determined in this study, and it is utilized to correct barrel distortion. The technique of

Least Mean Square Estimation (LMS) [4]. We reduced the square root operation. We present an algebraic manipulation method for reducing linear interpolation's arithmetic resource.

R - Rectangular coordinate.

P - Polar coordinate.

MRI - Magnetic Resonance Image.

CT - Computed Tomography.

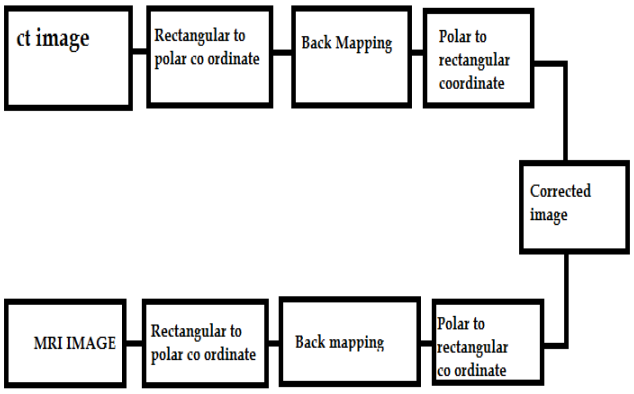

Fig.1. Distortion correction scheme

For image fusion, a deformed and noise-free image is provided. Even though there are a variety of ways for image fusion, we employ the discrete wavelet transform to fuse images [5]. For making use of picture fusion, this pixel transformation approach saves time and may be used with any software program. Digital filtering is used to produce the pixel time scales. The signal decomposed using high pass and low pass filters in the approximation technique. We're using two input photos (x 1 and x 2) that are overly fused together in this case. The raw images are then turned into wavelets using the HARR wavelet transform (W). The converted image coefficients are processed using a suitable fusion role to lower the noise level. Finally, to create a fused image, inverse wavelet transforms (W (-1)) are utilized.

As a result, each pixel in Distortion Image Space (DIS) is converted to Corrected Image Space (CIS), and the rectangle coordinate is converted to a polar coordinate. The "center of distortion" determines the distortion center. A distortion center (i_1', j_1') is known as a polar coordinate (r', Ø') in polar coordinate systems, and the distance r between a distortion center $(i_1, j_1)$and an image pixel (i', j') is expressed as,

$$r' = \sqrt{(i - i_1')^2 + (j' - j_1')^2} \quad (1)$$

$$\emptyset' = \arctan\left(\frac{j' - j_1'}{i' - i_1'}\right) \quad (2)$$

The distance r between the distortion centre (i, j) and the picture pixel is given by,

$$r = \sqrt{(i - i_1)^2 + (j - j_1)^2} \quad (3)$$

The angle formed by the pixel and the distortion center is,

$$\emptyset = \arctan\left(\frac{j - j_1}{i - i_1}\right) \quad (4)$$

Back-mapping is the second phase in our distortion process. The pixels (rØ', Ø') in the Corrected Image Spaces (CIS) are translated to the pixels (r',') in the Distortion Image Spaces (DIS). The link between 'r' and r degree N stated as is determined using an expansion polynomial.

$$r' = \sum_{n-1}^{N} c_n p'^n \quad (5)$$

$$\emptyset' = \emptyset \quad (6)$$

Because the expansion coefficient may be computed using nonlinear radial stretching [6], Around the distortion center, the distortion is regarded to be totally radial, with an equal angle. In Corrected Image Space (CIS), the new location (i', j') is computed as,

$$i = i_1 + r\cos\emptyset \quad (7)$$

$$j = j_1 + r\sin\emptyset \quad (8)$$

The third step involves transforming the polar coordinate into rectangular coordinates to correct the distortion in the processing approach. The alteration of the position ('i'', 'j'') in Distortion Image Spaces (DIS) is expressed as,

$$i' = i'_1 + r'\cos\emptyset \quad (9)$$

$$j' = j'_1 + r'\sin\emptyset \quad (10)$$

In Distortion Image Spaces, based on linear interpolation between intensity values of four nearest pixel ('i','j") in region (DIS).

A. Polar to Cartesian Coordinate Conversion and Back-Mapping Procedure

Back-mapping module translates pixel (r,) in CIS to its DIS equivalent ('r'',).

Here, N stands for polynomial degree.

$$r' = \sum_{n-1}^{N} d_n p'^n \quad (11)$$

$$\emptyset' = \emptyset \quad (12)$$

B. Analysis of Polynomial Approximation

It may be used to approximate the back-mapping expansion polynomial to polynomials of even or odd order.

$$r' = C_0 r + C_1 r^3 + C_2 r^5 + \cdots + C_n r^m \quad (13)$$

$$r' = Cb_0 r^2 + Cb_1 r^4 + \cdots . + Cb_1 r^o \quad (14)$$

Where, C_0, C_1, or CB_0, Cb_1, refers to the back-mapping polynomial with odd or even-order coefficients.

C. Back-Mapping Procedure Simplified

The odd-order polynomial may then be approximated using the back-mapping expansion polynomial.

$$r' = c_0 r + c_1 r^3 + c_2 r^5 + c_3 r^7 + \cdots \qquad (15)$$

The block diagram of the structural design is shown in

$$\sin \emptyset' = \sin \emptyset = \frac{j - j_1}{r} \qquad (16)$$

$$\cos \emptyset' = \cos \emptyset = \frac{i - i_1}{r} \qquad (17)$$

The square-root computation for r can be omitted because there are no odd powers of r in equation.

$$i' = i_1' + r' \frac{i - i_1}{r}$$

$$= i_1' + (c_0 r + c_1 r^3 + c_2 r^5 + c_3 r^7 + c_4 r^9 + \ldots) \times \frac{i - i_1}{r}$$

$$= i_1' + (c_0 + c_1 r^2 + c_2 r^4 + c_3 r^6 + c_4 r^8 + \ldots) \times (i - i_1)$$

$$j' = j_1' + r' \frac{j - j_1}{r}$$

$$= j_1' + (c_0 r + c_1 r^3 + c_2 r^5 + c_3 r^7 + c_4 r^9 + \ldots) \times \frac{j - j_1}{r}$$

$$= j_1' + (c_0 + c_1 r^2 + c_2 r^4 + c_3 r^6 + c_4 r^8 + \ldots) \times (j - j_1)$$

2. VLSI Architecture

The linear interpolation unit will have a 6-stage pipelined design, whereas the mapping unit will have a 15-stage pipelined architecture [8]-[13]. In rectified image spaces, the mapping unit will manipulate (‘u^', ‘^v') for each pixel (u, codetermine).

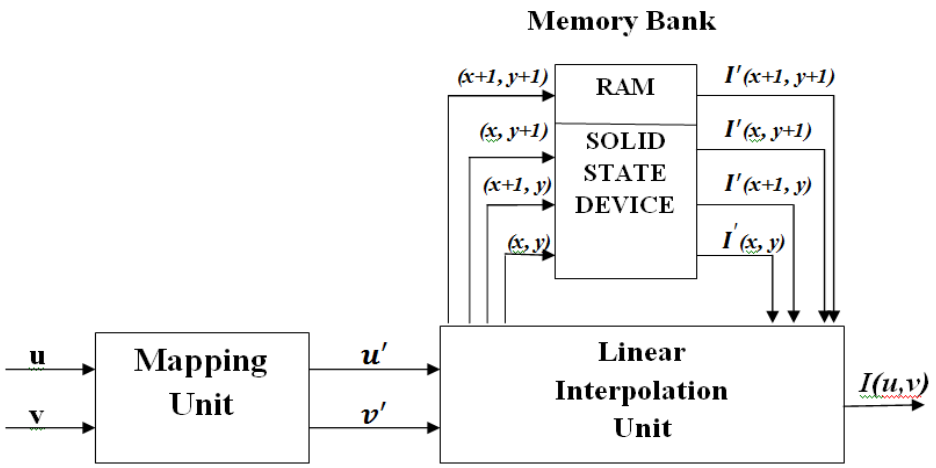

Fig.2. Proposed VLSI Architecture

In 15 stage pipelined architecture and 6 stage pipelined architecture we use 19 multipliers, 12 adders and 2 sub tractors.

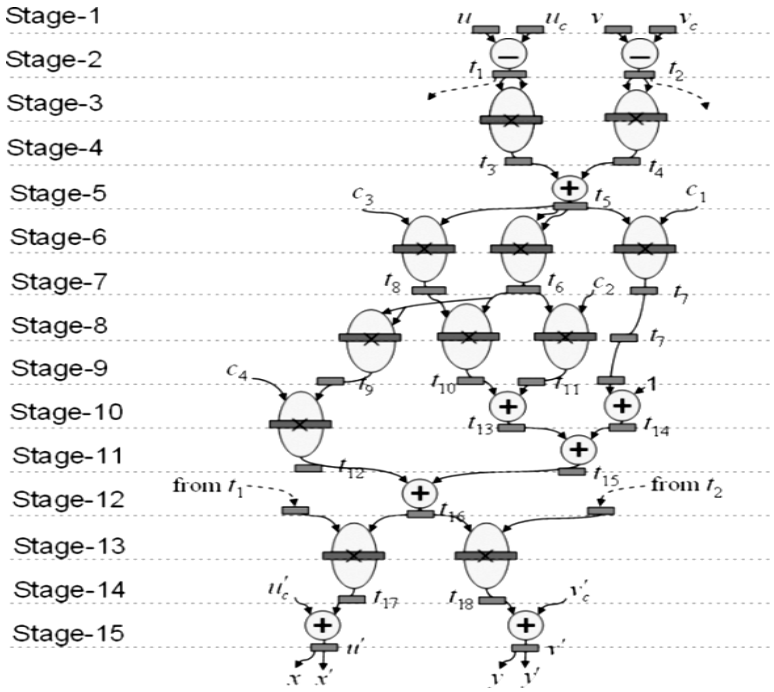

Fig.3. Map unit pipelined architecture

Most of the adders and multipliers are adopted 24-bit width [7]. The design structure formed to achieve high speed and less complexity,

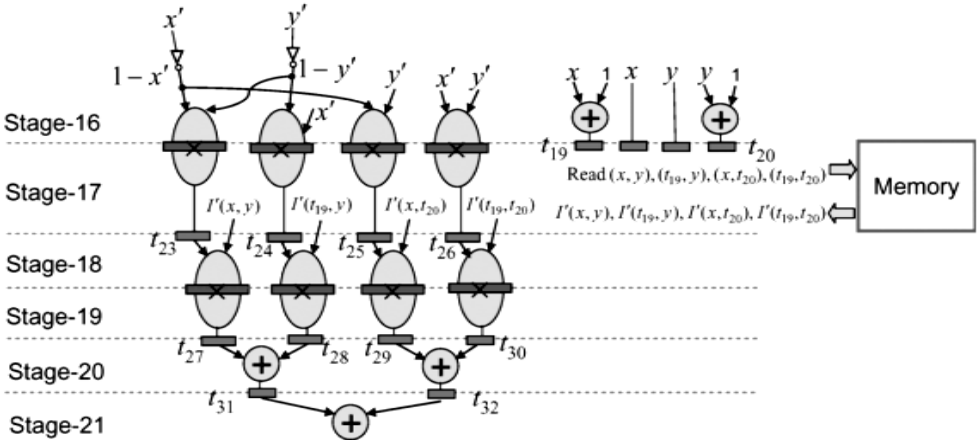

Fig.4. 6 stage pipelined architecture of Linear Interpolation unit

A. MATLAB DWT Architecture

The figure depicts the use of a DWT-based image fusion approach to create fused images from two (or) multiple photos. There is some imaging capability in this. The wavelet transform is used to convert the input signal into a time-frequency representation. The wavelet transform was created as a replacement for the short-time Fourier transform. We analyse dissimilar frequencies with numerous resolutions at different frequencies using the multi-resolution technique in wavelet transform. The suggested system reads images as text files. The MATLAB GUI interface is used to convert text files. Our DWT picture fusion uses filter banks calculated from discrete wavelet transforms to imitate the behaviour of continuous wavelet transforms. The pixels are sorted according to intensity using mathematical analysis after the signal has been processed using a filtering with a high and low pass. The K-Level decomposition in the wavelet transform has one low frequency component (LL band) and three high

frequency components (LH bands, HH bands, and HL bands). From the fusion of wavelet coefficients L, HL, HH, LH, an inverse discrete wavelet transform is utilised to rebuild the reconstructed fused image [9].

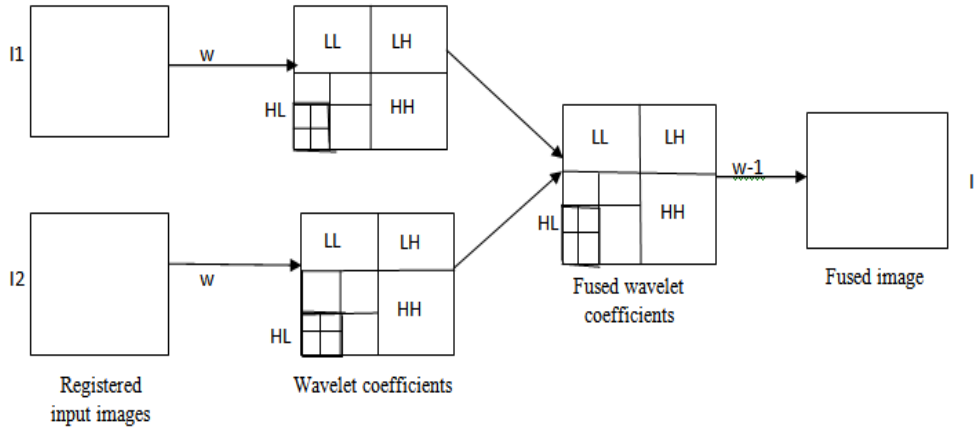

Fig.5. Scheme of image fusion using DWT

B. Results of Image Fusion

The fused images are made up of two (or more) different images. As a result, 3x3 matrices are used to track the images. The first three photos, mask (331), bust (332), and Catherine (333), are used as input images with (256x256) resolution (333). Figures (334) and (335) represent inputs of mask and bust, Figures (336) and (337), respectively, represent inputs of bust and Catherine, and Figures (338) and (339), respectively, represent the inputs of Catherine and mask. The mean-mean and max-min fusion rules are applied to the output. The output is in the form of a mean-mean and maximum-minimum synthesis.

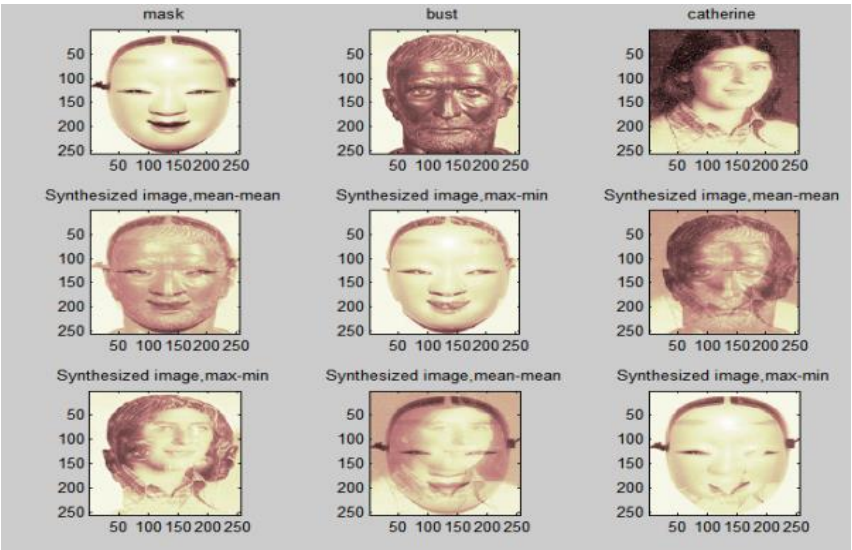

Fig.6. The output of image fusion

3. FPGA Implementation

The machine imports the raw image into the system. The programme that runs the system (i.e.) MATLAB GUI converts the image file into the text file. The text file then proposed with DWT. Our VLSI architecture gets this input for distortion correction.

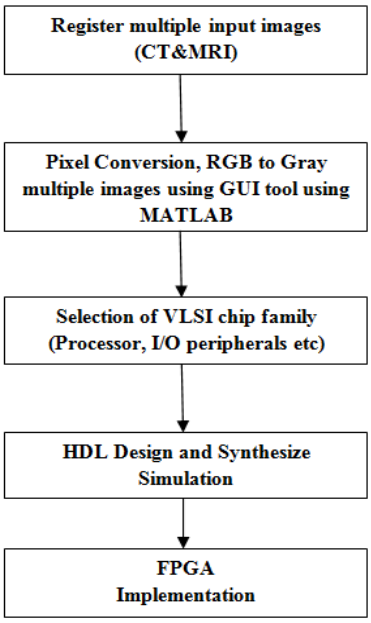

Fig.7. FPGA implementation process

4. Conclusion

The rigid image registration using wavelet based image fusion was performed using CT and MRI images. The quality of the images obtained by this technique has been verified using the Correlation Coefficient. The original input images and their corresponding registration and fusion results using the proposed technique are depicted in detail. The intensity based registration method was applied to the two input images, the quality of the registration was measured using the Correlation function to measure the similarity between the images before and after the registration the values of the correlation were displayed in percentage and the elapsed time taken for the registration process was also displayed, then the wavelet based image fusion algorithm was applied to the registered and reference images, the images were then decomposed and certain fusion rules were applied, finally the inverse decomposition was done to obtain the final fused images that contain information from both images. The quality of the fused images using the different fusion rules was done by measuring the Correlation Coefficient for each image fusion rule, and the resultant images are shown in the part of the result.

Declarations

Source of Funding

This research did not receive any grant from funding agencies in the public, commercial, or not-for-profit sectors.

Consent for publication

Authors declare that they consented for the publication of this research work.

References

[1] M. Mohankumar, V. Gopalakrishnan and S.Yasotha, (2015). A VLSI Approach for Distortion Correction in Surveillance Camera Images. ARPN Journal of Engineering and Applied Sciences, 10(9): 4105-4108.

[2] Yang, L., Wang, Y., Wang, Z. et al. (2020). A new method based on stacked auto-encoders to identify abnormal weather radar echo images. J Wireless Com Network 2020, 177. https://doi.org/10.1186/s13638-020-01769-3.

[3] M.Mohankumar, R.Gowrimanohari, (2015). VLSI Architecture for Barrel Distortion Correction In Surveillance Camera Images. Journal of Electronics and Computer Science, 2(5).

[4] Hareeta, M., Mahendra, K., Anurag, P. (2016). Image Fusion Based on the Modified Curvelet Transform. In: Unal, A., Nayak, M., Mishra, D.K., Singh, D., Joshi, A. (eds) Smart Trends in Information Technology and Computer Communications. SmartCom 2016. Communications in Computer and Information Science, vol 628. Springer, Singapore. https://doi.org/10.1007/978-981-10-3433-6_14.

[5] Al-Azzawi, N.A. (2018). Color Medical Imaging Fusion Based on Principle Component Analysis and F-Transform. Pattern Recognit. Image Anal. 28: 393-399. https://doi.org/10.1134/S105466181803001X.

[6] Wang, Hh. (2004). A New Multiwavelet-Based Approach to Image Fusion. Journal of Mathematical Imaging and Vision, 21: 177-192. https://doi.org/10.1023/B:JMIV.0000035181.00093.e3.

[7] Thamaraimanalan, T., RA, L., & RM, K. (2021). Multi Biometric Authentication using SVM and ANN Classifiers. Irish Interdisciplinary Journal of Science & Research, 5(1): 118-130.

[8] Das, S., Ghosh, S., Das, N. et al. (2018). Correction to: VLSI-Based Pipeline Architecture for Reversible Image Watermarking by Difference Expansion with High-Level Synthesis Approach. Circuits Syst Signal Process., 37, 5690. https://doi.org/10.1007/s00034-018-0979-1.

[9] Thamaraimanalan T, Sampath P (2019). A low power fuzzy logic based variable resolution ADC for wireless ECG monitoring systems. Cogn Syst Res., 57: 236-245. https://doi.org/10.1016/j.cogsys.2018.10.033.

[10] T. Thamaraimanalan and P. Sampath (2019). Leakage Power Reduction in Deep Submicron VLSI Circuits using Delay based Power Gating. National Academy Science Letters, 43(3): 229-232.

[11] Kidav, J.U., Ajeesh, P.A., Vasudev, D., Deepak, V.S., Menon, A. (2013). A VLSI Architecture for Wavelet Based Image Compression. In: Meghanathan, N., Nagamalai, D., Chaki, N. (eds) Advances in Computing and Information Technology. Advances in Intelligent Systems and Computing, vol 178. Springer, Berlin, Heidelberg. https://doi.org/10.1007/978-3-642-31600-5_59.

[12] Jonker, P.P. (1992). Pipelined low level image processing. In: Morphological Image Processing: Architecture and VLSI design. Springer, Boston, MA. https://doi.org/10.1007/978-1-4615-2804-3_5.

[13] Ranganathan, N., Nichani, S.J. & Mehrotra, R. (1991). A VLSI architecture for a half-edge-based corner detector. Machine Vis. Apps., 4: 165-181. https://doi.org/10.1007/BF01230199.